

# Geophysical Research Letters

## RESEARCH LETTER

10.1029/2020GL091374

### Key Points:

- Standard classifications of dimictic lakes do not consider how variable the initial thermal stratification can be under winter lake ice
- Lakes that are shallow or windy can cool to near 0°C–1°C before ice forms and are weakly stratified, which we term “cryomictic”
- Deeper lakes or those with calmer winds, result in ice forming just above deeper waters of 3°C–4°C, which we term “cryostratified”

### Supporting Information:

- Figure S1
- Table S1

### Correspondence to:

B. Yang and M. G. Wells,  
[bernie.yang@utoronto.ca](mailto:bernie.yang@utoronto.ca); [m.wells@utoronto.ca](mailto:m.wells@utoronto.ca)

### Citation:

Yang, B., Wells, M. G., McMeans, B. C., Dugan, H. A., Rusak, J. A., Weyhenmeyer, G. A., et al. (2021). A new thermal categorization of ice-covered lakes. *Geophysical Research Letters*, 48, e2020GL091374. <https://doi.org/10.1029/2020GL091374>

Received 26 OCT 2020

Accepted 16 DEC 2020

### Author Contributions:

**Conceptualization:** Bernard Yang, Mathew G. Wells, Hilary A. Dugan, James A. Rusak, Gesa A. Weyhenmeyer, Jennifer A. Brentrup, Allison R. Hrycik, Alo Laas, Rachel M. Pilla

**Formal analysis:** Bernard Yang

**Methodology:** Bernard Yang, Mathew G. Wells

**Resources:** Hilary A. Dugan, James A. Rusak, Gesa A. Weyhenmeyer, Jennifer A. Brentrup, Allison R. Hrycik, Alo Laas, Rachel M. Pilla, Jay A. Austin, Paul J. Blanchfield, Cayelan C. Carey, Matthew M. Guzzo, Noah R. Lottig, Murray D. MacKay, Trevor A. Middel, Don C. Pierson, Junbo Wang, Joelle D. Young

**Supervision:** Mathew G. Wells

## A New Thermal Categorization of Ice-Covered Lakes

Bernard Yang<sup>1</sup> , Mathew G. Wells<sup>1</sup> , Bailey C. McMeans<sup>2</sup> , Hilary A. Dugan<sup>3</sup> , James A. Rusak<sup>4,5</sup> , Gesa A. Weyhenmeyer<sup>6</sup> , Jennifer A. Brentrup<sup>7,8</sup> , Allison R. Hrycik<sup>7,9</sup> , Alo Laas<sup>10</sup> , Rachel M. Pilla<sup>11</sup> , Jay A. Austin<sup>12,13</sup> , Paul J. Blanchfield<sup>5,14</sup> , Cayelan C. Carey<sup>15</sup> , Matthew M. Guzzo<sup>2,16</sup> , Noah R. Lottig<sup>17</sup> , Murray D. MacKay<sup>18</sup> , Trevor A. Middel<sup>19</sup> , Don C. Pierson<sup>6</sup> , Junbo Wang<sup>20</sup> , and Joelle D. Young<sup>21</sup> 

<sup>1</sup>Department of Physical and Environmental Sciences, University of Toronto Scarborough, Toronto, ON, Canada,

<sup>2</sup>Department of Biology, University of Toronto Mississauga, Mississauga, ON, Canada, <sup>3</sup>Center for Limnology,

University of Wisconsin-Madison, Madison, WI, USA, <sup>4</sup>Dorset Environmental Science Centre, Ontario Ministry

of the Environment, Conservation, and Parks, Dorset, ON, Canada, <sup>5</sup>Department of Biology, Queen's University,

Kingston, ON, Canada, <sup>6</sup>Department of Ecology and Genetics/Limnology, Uppsala University, Uppsala, Sweden,

<sup>7</sup>Rubenstein Ecosystem Science Laboratory, University of Vermont, Burlington, VT, USA, <sup>8</sup>Department of Biology

and Environmental Studies, St. Olaf College, Northfield, MN, USA, <sup>9</sup>Department of Biology, University of Vermont,

Burlington, VT, USA, <sup>10</sup>Chair of Hydrobiology and Fishery, Institute of Agricultural and Environmental Sciences,

Estonian University of Life Sciences, Tartu, Estonia, <sup>11</sup>Department of Biology, Miami University, Oxford, OH,

USA, <sup>12</sup>Large Lakes Observatory, University of Minnesota Duluth, Duluth, MN, USA, <sup>13</sup>Department of Physics and

Astronomy, University of Minnesota Duluth, Duluth, MN, USA, <sup>14</sup>Fisheries and Oceans Canada, Winnipeg, MB,

Canada, <sup>15</sup>Department of Biological Sciences, Virginia Tech, Blacksburg, VA, USA, <sup>16</sup>Department of Integrative Biology,

University of Guelph, Guelph, ON, Canada, <sup>17</sup>Center for Limnology Trout Lake Station, University of Wisconsin-

Madison, Madison, WI, USA, <sup>18</sup>Environmental Numerical Weather Prediction Research, Science and Technology

Branch, Environment and Climate Change Canada, Toronto, ON, Canada, <sup>19</sup>Harkness Laboratory of Fisheries Research,

Aquatic Research and Monitoring Section, Ontario Ministry of Natural Resources, Trent University, Peterborough, ON,

Canada, <sup>20</sup>Key Laboratory of Tibetan Environment Changes and Land Surface Processes (TEL)/Nam Co Observation

and Research Station (NAMORS), Institute of Tibetan Plateau Research, Chinese Academy of Sciences, Beijing, China,

<sup>21</sup>Ontario Ministry of the Environment, Conservation, and Parks, Toronto, ON, Canada

**Abstract** Lakes are traditionally classified based on their thermal regime and trophic status. While this classification adequately captures many lakes, it is not sufficient to understand seasonally ice-covered lakes, the most common lake type on Earth. We describe the inverse thermal stratification in 19 highly varying lakes and derive a model that predicts the temperature profile as a function of wind stress, area, and depth. The results suggest an additional subdivision of seasonally ice-covered lakes to differentiate underice stratification. When ice forms in smaller and deeper lakes, inverse stratification will form with a thin buoyant layer of cold water (near 0°C) below the ice, which remains above a deeper 4°C layer. In contrast, the entire water column can cool to ~0°C in larger and shallower lakes. We suggest these alternative conditions for dimictic lakes be termed “cryostratified” and “cryomictic.”

**Plain Language Summary** Most mid and high latitude lakes are seasonally ice-covered and have only been classified based on the thermal structure and trophic status during the open-water season in summer. However, limited temperatures observations in these ice-covered lakes suggest that there is a wide range of thermal structures over winter. We developed an analytical model to predict the average water temperature at the time of ice formation based on the strength of the surface winds, the area of the lake, and the maximum depth of the lake. Using both the analytical model and water temperature data from 19 different lakes in North America, Europe, and Asia, we found that the time of ice formation in lakes that are large or experience strong winds were later compared to lakes that are small or experience weak winds. The larger and windier lakes are also colder (0°C~2°C) than smaller and calmer lakes (2°C~4°C) at the time of ice formation. This suggests that these seasonally ice-covered lakes can be subdivided into two additional classes during winter. The analytical model and the new categorization have important consequences for understanding fish habitat under the ice and the potential effects of climate change on these seasonally ice-covered lakes.

**Writing – original draft:** Bernard Yang, Mathew G. Wells, Bailey C. McMeans

**Writing – review & editing:** Bernard Yang, Mathew G. Wells, Bailey C. McMeans, Hilary A. Dugan, James A. Rusak, Gesa A. Weyhenmeyer, Jennifer A. Brentrup, Allison R. Hrycik, Alo Laas, Rachel M. Pilla, Jay A. Austin, Paul J. Blanchfield, Cayelan C. Carey, Matthew M. Guzzo, Noah R. Lottig, Murray D. MacKay, Trevor A. Middel, Don C. Pierson, Junbo Wang, Joelle D. Young

## 1. Introduction

At least 50% of the lakes in the world are located at high latitudes and are seasonally ice-covered (Verpoorter et al., 2014). Therefore, it is important to understand the broad controls on thermal stratification present during winter in these ubiquitous dimictic lakes at temperate and boreal regions. In dimictic lakes, the water column becomes thermally stratified under lake ice in the winter. While considerable effort has been made to describe the details of summer thermal stratification in dimictic lakes (e.g., Boehrer & Schultze, 2008), most textbooks do not go much beyond saying that during winter an inverse stratification exists (e.g., Wetzel, 2001), following the original classification scheme of dimictic lakes by Lewis (1983). In this lake classification scheme, only four examples of dimictic lakes are given, of which only two lakes (Lake Erken in Sweden and Lake Mendota in Wisconsin, United States of America) were not meromictic. It is unclear, however, to what degree these two lakes should be considered archetypes of winter conditions in all dimictic lakes. In particular, the strength of thermal stratification and mixing that occurs before and during ice formation remains unknown, as underice processes have been reported in only 2% of the peer-reviewed literature on freshwater systems (Hampton et al., 2015, 2017). Once ice onset occurs in dimictic lakes, the initial thermal stratification present during ice formation largely persists through the whole winter prior to the late-winter convection period (Bruesewitz et al., 2015; Yang et al., 2017, 2020; MacKay et al., 2017). The resulting underice thermal profile regulates biological activity, as both a habitat for fish (McMeans et al., 2020) and plankton (Kelley, 1997; Hampton et al., 2015). It also influences lake hydrodynamics, through control on internal waves, circulation, and vertical mixing (Kirillin et al., 2012). Consequently, determining the drivers of underice thermal stratification in dimictic lakes is needed to better understand underice conditions as they rapidly change (Hampton et al., 2017), especially as lakes are warming under a changing climate (O'Reilly et al., 2015).

The extent of surface mixing after the water column cools to 4°C and before ice forms in the fall or early winter controls the heat distribution through the water column and influences the thermal stratification at ice-on (Figure 1). The mixing dynamics are determined by the nonlinear equation of state, where freshwater becomes less dense as temperature decreases below 4°C. Therefore, cooling that occurs above 4°C destabilizes the water-column, whereas surface cooling below 4°C is a stabilizing buoyancy flux that restratifies the water column. In general, lakes subjected to more intense wind mixing during late fall will have lower water column temperatures, so that wind speed prior to ice formation should determine early winter temperature profiles (Farmer & Carmack, 1981). Using the idea of a one-dimensional Monin-Obukhov scaling, Farmer and Carmack (1981) suggested that a vertical length scale for the cold buoyant layer is  $H_{FC} \sim u_*^3 / B$ , where  $u_*$  is the friction velocity and  $B$  is the buoyancy flux per unit area. Hence, stronger winds result in a deeper cold layer before ice-on (Figures 1a and 1c), whereas calmer lakes have shallower cold surface layers (Figures 1b and 1d). The local wind stress experienced between nearby lakes can vary (Read et al., 2012), depending upon local topography and the influence of wind sheltering (Markfort et al., 2010). These effects mean that larger lakes have stronger winds (i.e.  $u_* \sim L$ ), when compared to nearby lakes of smaller area. The same balance between vertical mixing and a stable buoyancy flux applies to the summer thermocline, and a similar Monin-Obukhov scaling argument has been used by Kirillin and Shatwell (2016) to separate the summer stratification of 378 lakes into polymictic or stratified dimictic systems.

The physics of inverse stratification prior to formation of ice cover is analogous to the widely studied process of thermocline formation in early summer in dimictic lakes. For instance, the depth of a dimictic lake's thermocline can also be related to the magnitude of wind-driven mixing and the lake's geometry. Gorham and Boyce (1989) used a two-dimensional argument based on the Wedderburn number to show that the depth of the late summer thermocline scaled as

$$H_{GB} \sim \bar{u}_* \sqrt{L / g'} \quad (1)$$

where  $\bar{u}_*$  is the friction velocity averaged over the summer stratified period,  $L$  the fetch and  $g'$  the reduced gravity across the thermocline, defined as  $g' = g \Delta\rho / \rho_o$ , where  $g$  is the gravitational acceleration,  $\Delta\rho$  is the density difference across the thermocline, and  $\rho_o$  is the average density of the water column. In contrast to the one-dimensional Monin-Obukhov scaling used by Farmer and Carmack (1981) and Kirillin and Shatwell (2016), this scaling is a steady state scaling and explicitly includes the effects of the lake geometry,

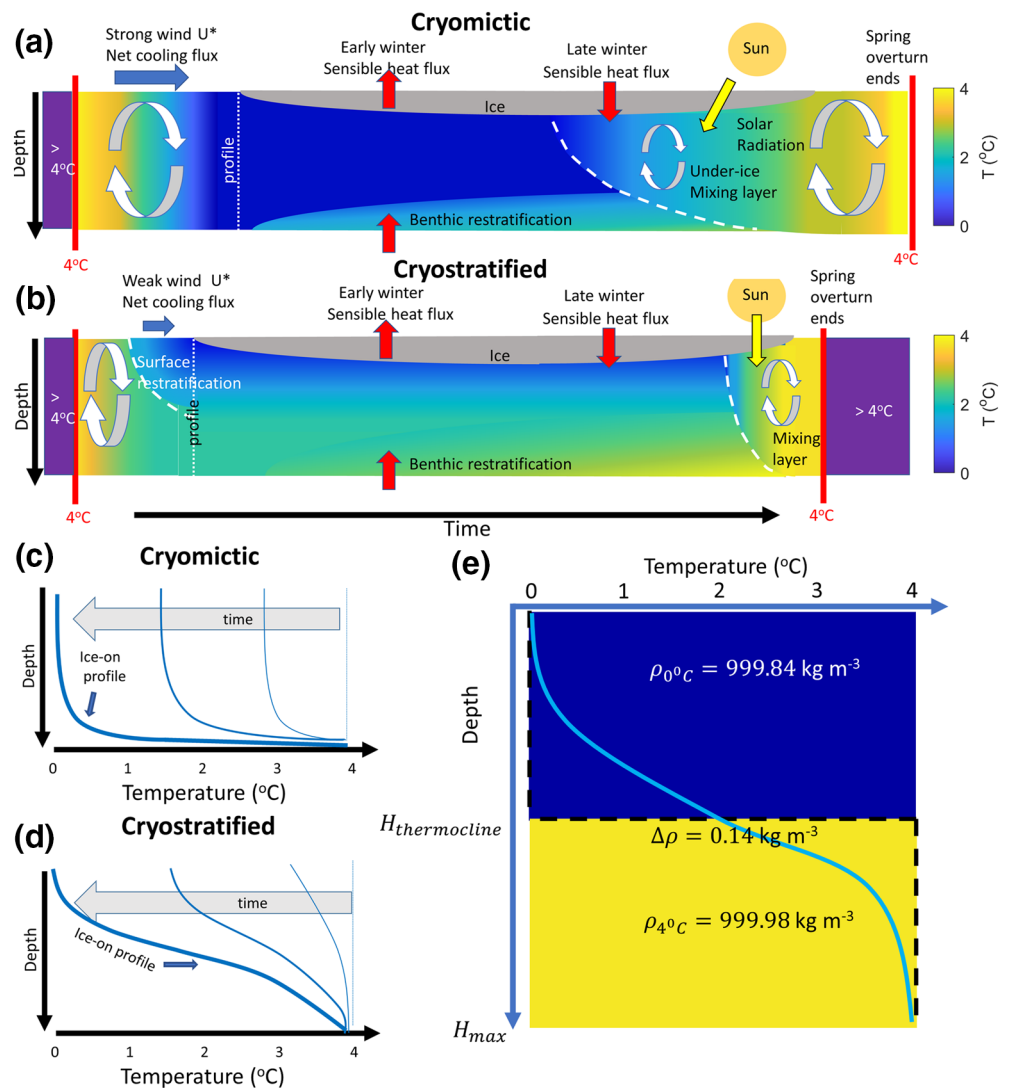


**Figure 1.** Schematic showing the difference in thermal structure between (a) a wide, shallow, and windy lake with a deeper cold layer and weak stratification, and (b) a small, deep, and calm lake with strong inverse stratification. Corresponding evolution of temperature profiles until ice-on for (c) wide lake and (d) small lake. (e) An idealized schematic of winter thermocline depth  $H_{thermocline}$  used to develop our theory with the black dashed line showing the vertical temperature profile for the idealized two-layer model and the blue curve as an example of an actual vertical temperature profile.

namely the fetch of the lake. The scaling of Gorham and Boyce (1989) does not explicitly include the complex relationship between buoyancy fluxes and surface winds captured by the Monin-Obukhov scaling used by Farmer and Carmack (1981). Nevertheless, Gorham and Boyce found a good agreement with their prediction when looking at end-of-summer thermocline depths  $H$  in 150 lakes. Fee et al. (1996) found that  $H$  during midsummer had a positive correlation with  $A^{\frac{1}{4}}$ , where  $A$  is the surface area of the lake. If the lake is circular, then  $A^{\frac{1}{4}} \sim L^{\frac{1}{2}}$ . For a fixed wind speed, this is the same scaling relationship as  $H_{GB} \sim L^{\frac{1}{2}}$  obtained by Gorham and Boyce (1989). Both the one and two-dimensional arguments suggest that with more wind, the thermocline during the formation of stratification in a dimictic lake becomes deeper, a result that applies to both early summer and early winter. However, this scaling has never been applied to winter conditions before.

Despite the extensive work published on quantifying the relative contributions of surface momentum flux to buoyancy flux in establishing the summer dynamics, there is no comparable work on the fall overturn period establishing the underice stratification, likely because winter field work has substantial logistical challenges (Block et al., 2019). In this analysis, we use temperature and wind speed data from 19 lakes across North America, Europe, and Asia to explore the degree to which winter thermal stratification in ice-covered lakes is controlled by wind. Using these results, we suggest that the traditional classification by thermal regime and trophic status is not sufficient to understand the early winter stratification in ice-covered lakes. We provide an additional categorization for ice-covered lakes based on the thermal stratification patterns across the different lakes in the study: cryomictic for lakes that are cold and mixed at ice-on, and cryostratified for lakes that are warmer and stratified at ice-on. This additional categorization has broad implications for our understanding of underice thermal conditions in lakes.

## 2. Study Sites and Data

To classify the thermal profiles of lakes over a range of geographic locations with different climatic conditions, we used continuous water temperature measurements from 19 lakes across North America, Northern Europe, and Asia. This dataset covers a broad range of surface areas and maximum depths (Figure S1; Table S1). We defined the start of the inverse stratification period as when the vertically averaged water temperature was 4°C, close to the temperature of maximum density of freshwater (Chen & Millero, 1986), and we defined the timing of ice-on as the day of full ice cover. In larger lakes that are often partially ice-covered, we defined the timing of ice-on to be the first day where at least a radius of 10 km from the sampling point is ice-covered, which is consistent with the definition used in Titze and Austin (2016) (Table S1). In all lakes, water temperature was measured continuously at multiple depths (Table S1). Out of the 19 lakes in this study, 13 lakes included hourly wind speed measurements near the surface of the lake. Detailed lake characteristics and sampling details are given in Table S1.

### 2.1. Calculating Depth Averaged Temperatures

The depth-averaged temperature  $T_{\text{avg}}$  was calculated at the time of reported ice-on. We first calculated the temporal average of the vertical temperature profiles from 2 days before the onset of ice cover to 2 days after. In many cases, the moorings did not extend to the surface, due to vulnerability of the instruments to the lake ice, and instead the shallowest thermistors were typically below ice at 0.5 to 2 m depth. In these cases, we assumed that  $T = 0$  at  $z = 0$ , and made a linear interpolation between that and the highest measurement. We also assumed that the temperature at the bottom was equal to the temperature at the deepest logger. Typically, this represents a slight underestimation of the actual depth-averaged temperature due to the inverse thermal stratification in cold lakes. However, there are special cases where compressibility effects were significant in very deep lakes (e.g. Lake Superior), resulting in an overestimation of the depth-averaged temperature at ice-on.

### 2.2. Calculating Time Averaged Winds and the Drag Coefficient

For each lake, we determined the average surface wind at 10 m above the surface of the lake,  $U_{10}$ , by averaging the wind speeds between the start of inverse stratification and onset of ice cover. In cases where the wind measurements were made at another height  $z$ , we used a power-law scaling formula to estimate  $U_{10}$  following Hsu et al. (1994):

$$U_{10} = U_z \left( \frac{10}{z} \right)^{0.11}$$

where  $U_z$  is the wind measured at height  $z$  above the surface of the lake. To account for the variability of the wind measurements during this period, we calculated the sample standard deviation of all the wind speeds to obtain the wind speeds at the 25<sup>th</sup> and the 75<sup>th</sup> percentile that were used to construct the error bars.

The drag coefficient  $C_{D,10}$  was calculated using Charnock's Law (Charnock, 1955) and the empirical relationship determined by Wüest and Lorke (2003)

$$C_{D,10} = \begin{cases} 0.0044U_{10}^{-1.15}, & U_{10} < 5 \text{ m s}^{-1} \\ \left[ \kappa^{-1} \ln \left( \frac{10g}{C_{D,10}U_{10}^2} \right) + 11.3 \right]^{-2}, & U_{10} > 5 \text{ m s}^{-1} \end{cases}$$

where  $\kappa$  is the von Karman constant and  $g$  is the gravitational acceleration.

### 3. Modeling Approach

#### 3.1. Modeling the Water Temperature at Ice Formation Based on Wind Measurements and Geometry of the Lake

The average temperature at ice-on can be estimated from a highly simplified two-layer model that has a top layer of thickness  $H_{\text{thermocline}}$  and a total depth of  $H_{\text{max}}$ , where the temperature is set to  $0^\circ\text{C}$  above the winter thermocline and  $4^\circ\text{C}$  below (Figure 1e). The depth averaged temperature of a lake at ice-on in degrees Celsius can be calculated as

$$\hat{T}_{\text{ice-on}} = \frac{1}{H_{\text{max}}} (0 \times H_{\text{thermocline}} + 4 \times (H_{\text{max}} - H_{\text{thermocline}}))$$

which simplifies to

$$\hat{T}_{\text{ice-on}} = 4 \left( 1 - \frac{H_{\text{thermocline}}}{H_{\text{max}}} \right) \quad (2)$$

We define the depth of the thermocline based on the results of Gorham and Boyce (1989), who modeled the full scaling of the thermocline depth based on wind driven mixing events as

$$H_{\text{thermocline}} \equiv H_{GB} = 2 \left( \frac{\tau}{g\Delta\rho} \right)^{\frac{1}{2}} A^{\frac{1}{4}} \quad (3)$$

where  $\tau$  is the surface wind stress,  $A$  is the surface area of the lake, and  $\Delta\rho$  is the density difference between the two layers. The surface wind stress is given by

$$\tau \equiv \rho_w u_*^2 = \rho_a C_{D,10} U_{10}^2 \quad (4)$$

where  $\rho_w$  is the density of water (taken to be  $1,000 \text{ kg m}^{-3}$  here),  $\rho_a$  is the density of air ( $1 \text{ kg m}^{-3}$ ),  $U_{10}$  is the wind speed measured 10 m above the surface of the lake, and  $C_{D,10}$  is the drag coefficient for surface winds at 10 m. The thermocline scaling of Gorham and Boyce (1989) is consistent with previous arguments about mixing of stratified lakes in context of a Wedderburn number defined as  $W = \frac{g'h^2}{u_*^2 L}$  (Spiegel & Imberger 1980; Coman & Wells 2012). The empirical coefficient of 2 in Equation 3 is then equivalent to a condition that the time averaged  $W$  is 4.

Combining Equations 3–5, the depth of the thermocline can be written as

$$H_{\text{thermocline}} = 2 \left( \frac{\overline{u_*^2}}{g'} \right)^{\frac{1}{2}} A^{\frac{1}{4}} \quad (5)$$

where  $g'$  is the reduced gravity defined in terms of the density difference between  $0^\circ\text{C}$  and  $4^\circ\text{C}$  water as  $g' = g(\rho_{4^\circ\text{C}} - \rho_{0^\circ\text{C}}) / 0.5(\rho_{4^\circ\text{C}} + \rho_{0^\circ\text{C}})$ , and the overbar indicates temporal averaging from the start of the inverse stratification period to the onset of ice formation. Using this, we obtain a novel estimation of the depth-averaged temperature at ice-on based on both the surface winds over the lake and the geometry of the lake by substituting into Equation 2

$$\hat{T}_{\text{ice-on}} = \max \left\{ 0, 4 \left( 1 - \frac{\overline{2u_* g' \frac{1}{2} A^{\frac{1}{2}}}}{H_{\text{max}}} \right) \right\} \quad (6)$$

## 4. Results

### 4.1. Detailed Comparison of Thermal Stratification During the Fall and Winter Between a Small and Large Lake

Our new modeling approach suggests that local wind and lake area have important roles in determining the thermal profile at ice formation, and the extent to which dimictic lakes can vary between being cryomictic and cryostratified. This difference in thermal profiles is seen most clearly when comparing Lake Mendota (surface area 39.6 km<sup>2</sup>) with Harp Lake (surface area 0.714 km<sup>2</sup>). These lakes have similar maximum depths (25–30 m) and are at approximately the same latitude (43°N–45°N) in mid-continental North America, thus experience similar air temperatures and solar radiation. The most important difference between the lakes is the wind they experience. The average wind  $U_{10}$  on Lake Mendota at the start of the inverse stratification period and prior to ice-on was 5.8 m s<sup>-1</sup>, whereas the average  $U_{10}$  was only 0.9 m s<sup>-1</sup> prior to ice formation in Harp Lake. Consequently, temperature profiles of the two lakes at the time of initial ice formation were different, which influenced the stratification pattern during winter. During the early winter of 2019 between ice-on and February 1 in Lake Mendota, the water column was nearly isothermal. Before the surface-mixing layer started to develop in late March, most of the upper water column remained close to isothermal. Beneath the isothermal upper layer, the temperature was increasing at approximately 0.15°C m<sup>-1</sup>, and the strongest stratification was at the bottom of the lake where the temperature increased at 0.5°C m<sup>-1</sup>. In contrast, Harp Lake had only a thin surface layer near the surface that was less than 3°C. This surface layer was less than 3 m thick and strongly stratified where the maximum temperature gradients were 1.5°C m<sup>-1</sup>. Beneath this strongly stratified layer, the water column was between 3°C and 4°C and the temperature gradients did not exceed 0.1°C m<sup>-1</sup>.

### 4.2. Comparison of Water Temperature at Ice-On with Lake Size and the Strength of Surface Winds

Extending the observations to 19 lakes globally, our data show that the ice-on temperature profiles vary widely (Figure 3a). Lake Erie had the coldest temperature at ice-on at nearly 0°C and was nearly isothermal. The temperature profiles in other larger lakes such as Lake Simcoe were less than 1°C in the upper half of the water column, and between 1°C and 2°C near the bottom of the lake. In contrast, in other smaller lakes such as Alexie Lake, the water column at mid-depths were greater than 2°C and the temperature near the bottom can be close to 4°C, the temperature of maximum density.

We found a strong relationship between the surface winds and the depth-averaged ice-on temperatures. Lakes that experience weaker surface winds prior to ice-on had higher average temperatures at ice-on, while stronger winds led to lower average temperatures at ice-on (Figure 3b). This is consistent with stronger winds driving a deeper surface mixing layer prior to ice-on that transports colder waters to the bottom. The ice-on temperatures of each lake also appear to be well-correlated to the aspect ratio of the lake  $H_{\text{max}} / \sqrt{A}$ , where  $A$  is the surface area of the lake. This value is high for small, deep lakes and low for large, shallow lakes (Figure 3c). In general, we found that a larger surface area of the lake corresponds to higher average strength of the surface winds (Figure 3d). The temperature scaling using our new idealized two-layer model (Equation 6) agreed very well with the measured average temperature during ice-on (Figure 3e).

## 5. Discussion

Our synthesis of data from 19 lakes in North America, Europe, and Asia suggests that there is a large variation of ice-on temperature profiles between cryomictic and cryostratified, and that mean ice-on temperatures were well-predicted by lake depth, area and wind stress prior to ice-on (Equation 6). For lakes

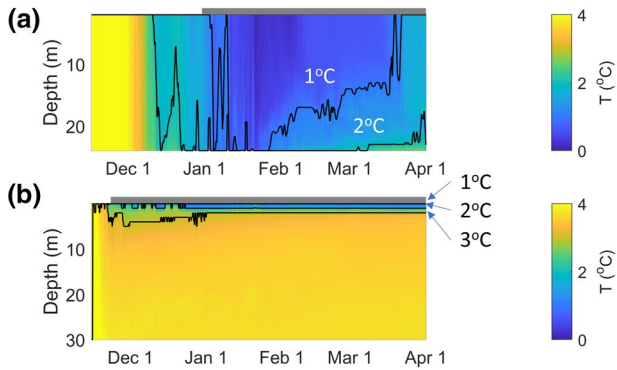


**Figure 2.** Difference in thermal structure between (a) Lake Mendota (a large lake, 43.1°N), and (b) Harp Lake (a small lake, 45.3°N) during the winter of 2019. These two lakes are at a similar latitude yet the thermal stratification in Lake Mendota was weak and colder compared to Harp Lake. While the Harp Lake site is 36 m deep, data are only shown for the top 30 m where continuous measurements were taken. In both plots, the gray bar on top of both plots indicate the duration of ice cover.

without available wind data, the depth-averaged temperature at ice-on correlated well with  $\log(H_{\max} / \sqrt{A})$ , where larger values indicate a deeper lake relative to its surface area. We emphasize that although the correlation coefficients  $R_{\text{adj}}^2$  are similar between comparing  $T_{\text{ice-on}}$  against  $\log(H_{\max} / \sqrt{A})$  ( $R_{\text{adj}}^2 = 0.644$ , Figure 3c) and comparing  $T_{\text{ice-on}}$  against  $\hat{T}_{\text{ice-on}}$  ( $R_{\text{adj}}^2 = 0.753$ , Equation 6, Figure 3e), the new two-layer model scaling is based on the essential physics of the mixing layer depth proposed by Gorham and Boyce (1989) during wind events. However, if the surface winds (friction velocity) can be assumed to be an increasing function of  $\sqrt{A}$  (Figure 3d), then Equation 6 suggests that  $\hat{T}_{\text{ice-on}}$  will be a function of the vertical aspect ratio  $H_{\max} / \sqrt{A}$  (Figure 3c). Here, we found that most cryostratified lakes at ice-on have larger values of  $\log(H_{\max} / \sqrt{A})$  and have weaker winds (Figure 3c).

More generally, the data and Equation 6 suggest that the initial underice winter thermal stratification of a dimictic lake is best characterized by a gradient - on one end the depth-averaged temperatures are “cold” and close to 0°C with near uniform temperatures in a weakly stratified lake, whereas at the other end, the lake is “warm” with a thin cold layer of water

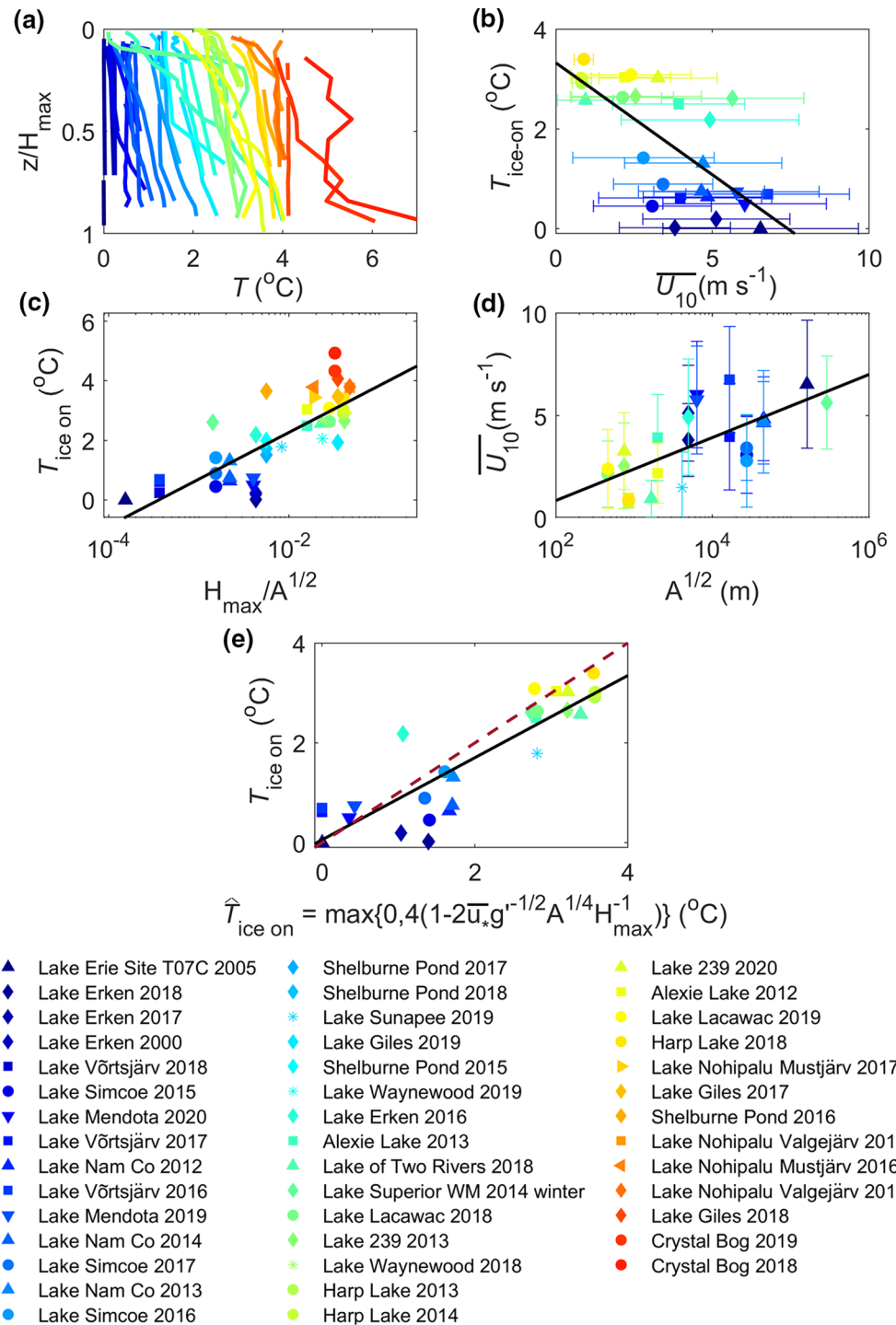
immediately beneath the ice and then a deep layer of water that is near 4°C. In light of this, we suggest that it is useful to further subdivide the dimictic classification scheme of Lewis (1983) into additional categories and that the term “inverse stratification”, when applied widely to characterize seasonally ice-covered lakes, may be misleading in many cases. We suggest that a new term “cryostratified” lakes be used when the depth-averaged initial winter temperature is between 2°C and 4°C under the ice (e.g. Harp Lake, Figure 2b), and the term “cryomictic” lakes be used where depth-averaged temperatures are between 0°C and 2°C (e.g., Lake Mendota, Figure 2a). In the absence of additional chemical stratification, all initial underice winter temperature profiles exist on a continuum between these states. The use of these new terms will be helpful when comparing different lakes regarding fish habitat usage over winter or advancing our understanding of underice dynamics in lakes.

### 5.1. Implications of the New Categorization System for Biological Processes

The division of lakes into cryostratified and cryomictic may help to better understand the abundance of fish. Fish are ectotherms, so their use of different thermal habitat in a stratified water column has implications for their physiological rates and performance (Huey, 1991). Freshwater fish are known to select habitats that align with their thermal preferences (Brandt et al. 1980). However, fish habitat choice in winter, when temperatures range from near 0°C just below ice to near 4°C at the bottom, is poorly understood. Both winter inactive (e.g. smallmouth bass, Suski & Ridgway, 2009) and winter active (e.g. burbot; Harrison et al., 2016) fish species appear to select for particular depths during winter, and a number of studies on salmonids suggest that these cold-adapted fish often occupy higher and colder regions of the water column in a narrow depth range during winter that corresponds to temperatures between 1°C and 3°C (Bergstedt et al., 2003; Blanchfield et al., 2009; McMeans et al., 2020; Cote et al., 2020). If fish are indeed choosing a specific 2°C isotherm, this layer would be deeper in cryomictic lakes. For instance, the 2°C isotherm is at approximately 90% of lake depth in the colder Lake Mendota, versus approximately 5% depth in Harp Lake (Figure 2). The degree to which differing winter stratification patterns drive different depth usage by fish, and the consequences for fish growth and survival, would therefore be a valuable research topic for future telemetry studies.

### 5.2. Implications of the New Categorization for Underice Physical Processes

Initial differences in thermal stratification under the ice influence late winter stratification, and can subsequently influence the magnitude of two key physical processes, namely (1) the duration and strength of



vertical heat fluxes associated with the late winter radiatively driven convection, and (2) the timing and duration of spring overturn dynamics (Figure 1).

The duration and strength of late-winter convection and spring overturn depend on the buoyancy flux from solar radiation and the depth of the surface mixed layer, and could vary widely between different lakes even of similar size (Bruesewitz et al., 2015; Forrest et al., 2013). In cryostratified lakes, there is strong stratification near the surface so that there is a very thin surface mixed layer. In contrast, a small increase in under ice temperatures from solar heat can potentially trigger convective mixing throughout a large region of the water column in cold cryomictic lakes that are weakly stratified (Bruesewitz et al., 2015; Yang

et al. 2020). Similarly, the vertical velocities associated with solar-driven convection scale as  $w^* \sim (Bh)^{\frac{1}{3}}$  (Bouffard et al., 2019; Kelley, 1997), where  $B$  is the buoyancy flux, and  $h$  is the depth of the surface mixed layer. It is likely that  $h$  is larger in cryomictic lakes during underice convection, and therefore more likely to have larger vertical velocities  $w^*$  and stronger convection under the ice. The degree of convection may in turn structure the planktonic communities (Bouffard et al., 2019; Kelley, 1997) as plankton rely on the vertical circulation to remain in the photic zone (Yang et al., 2020). In very large and deep lakes such as Lake Superior and Lake Michigan, the spring overturn can continue for weeks to months after ice-off, until the water column reaches 4°C (Austin, 2019; Cannon et al., 2019). However, under similar meteorological forcing, we would expect that cryostratified lakes, such as Harp Lake (Figure 2b), will warm up to 4°C faster than colder cryomictic lakes after ice-off, and consequently have a shorter duration of spring overturn (Yang et al., 2020).

Furthermore, both the data from 19 lakes (Figure 3e) and the Equation 6 suggest that the temperature at ice formation may be sensitive to shifts in surface winds. In particular, ice-on temperatures in larger lakes are more sensitive to differences in surface winds as Equation 6 implies that  $\left| \frac{\partial T_{\text{avg}}}{\partial u_*} \right| = 8g'^{-\frac{1}{2}} A^{\frac{1}{4}} H_{\text{max}}^{-1}$  is greater for shallow lakes with larger area (see example in Figure s2). In some locations surface winds have increased by 10%–20% recently (e.g. over Lake Superior, Desai et al., 2009), while in other locations winds have dropped by 10%–20% (Pryor et al., 2009; Vautard et al., 2010). Such shifts in the mean surface winds or variability with late fall storm events on lakes that have ice-on temperatures that are close to 2°C might shift lakes between cryomictic and cryostratified states, depending on the surface winds. This dependence on wind speed in Equation 6 highlights a potential problem of using just the simple regression to lake geometry shown in Figure 3c.

### 5.3. Limitations of the Analysis

The main assumption we have made in our analysis is that the thermal stratification at ice-on is primarily determined by surface heat fluxes and the turbulent mixing is driven by winds. Other processes could be important in setting the winter thermal stratification. For example, the timing of ice formation is not explicitly addressed our temperature scaling (Equation 6). Deeper lakes have a later time of ice formation after the surface cools to 0°C (Kirillin et al., 2012), which potentially allows for more cooling of the lake. River inflows can impact the thermal stratification and chemical stratification (Cortés & MacIntyre, 2019; Pasche et al., 2019), which will be important in lakes that have short residence times. The summer heat stored in the sediment can also be an important source of heat fluxes in lakes that have significant shallow zones (Fang & Stefan, 1996, 1998). Finally, in very deep lakes, such as Lake Superior, compressibility effects are important, so that stable temperature profiles follow a thermobaric relationship, rather than strictly increasing with depth (Boehrer & Schultze, 2008; Crawford & Collier, 2007; Titze & Austin, 2014). This implies that the depth averaged temperature of a deep lake at ice-on might be lower than expected based on similar shallow lakes.

**Figure 3.** Water temperatures in our study lakes, each denoted by a unique color/symbol combination: (a) Temperature profiles of each lake at ice-on with depth ( $z$ ) on the y-axis normalized by the maximum depth of each lake ( $H_{\text{max}}$ ). (b) Relationship between depth-averaged temperature at ice-on ( $T_{\text{ice-on}}$ ) compared to  $\bar{U}_{10}$ , which, for lakes with wind data, was averaged from when the water column cooled to 4°C to ice-on. (c)  $T_{\text{ice-on}}$  compared to the ratio of the maximum depth ( $H_{\text{max}}$ ) and the square root of the lake surface area ( $A^{\frac{1}{2}}$ ). (d)  $\bar{U}_{10}$  during the same period in (b) compared to  $A^{\frac{1}{2}}$ . (e) Observed  $T_{\text{ice-on}}$  compared to  $\hat{T}_{\text{ice-on}}$  (Equation 6) with the dashed line representing 1:1. The black lines indicate the linear regressions for (b)  $T_{\text{ice-on}} = 3.32 - 0.45\bar{U}_{10}$ ,  $R_{\text{adj}}^2 = 0.463$ , slope  $p < 0.01$ , (c)  $T_{\text{ice-on}} = 5.41 + 0.68 \log(H_{\text{max}} A^{-1/2})$ ,  $R_{\text{adj}}^2 = 0.644$ , slope  $p < 0.0001$ , (d)  $\bar{U}_{10} = -2.23 + 0.67 \log(A^{1/2})$ ,  $R_{\text{adj}}^2 = 0.43$ , slope  $p < 0.001$ , and (e)  $T_{\text{ice-on}} = 0.06 + 0.82 \hat{T}_{\text{ice-on}}$ ,  $R_{\text{adj}}^2 = 0.753$ , slope  $p < 0.001$ . Red colors indicate warmer  $T_{\text{ice-on}}$  and blue colors indicate colder  $T_{\text{ice-on}}$ . The error bars on (b) and (d) indicate the standard deviation of  $U_{10}$  from the start of the inverse stratification period to the time of ice formation.

## 6. Conclusions

Although Lewis (1983) originally classified all dimictic lakes into one group, we conclude that dimictic lakes should further be differentiated into cryostratified and cryomictic. We suggest that smaller lakes with less wind result in “warmer” underice temperatures near 4°C and should be termed “cryostratified” whereas larger lakes with higher winds are typically “colder” (near 0°C) and should be termed “cryomictic”. Stronger winds at the surface potentially drive a longer duration of mixing by delaying ice formation (Kirillin et al., 2012), and hence the temperature profiles at ice-on are colder and more isothermal compared to lakes with weaker winds. We developed an equation that predicts the mean temperature at ice-on from the wind speed and lake geometry (Equation 6) and compares well with measurements from our study lakes. In cases where surface wind measurements are not available, the nondimensional ratio  $\log(H_{\text{mean}} / \sqrt{A})$  correlates well with the mean ice-on temperature. These results suggest that there is a wide spectrum of ice-on temperature profiles in temperate, dimictic lakes. Furthermore, we expect similar processes will occur in high latitude polymictic lakes or cold monomictic lakes. For example, Lake Vörtsjärv and Shelburne Pond were two polymictic lakes included in the analysis. Greater recognition and better characterization of the variability in thermal structure under the ice will have important implications for understanding both the ecology and physical dynamics of dimictic lakes during winter.

## Data Availability Statement

References of all previously published data are available in Table S1 (Cott et al. 2015; Guzzo et al. 2016; LSPA et al., 2020; MacKay et al., 2017; McMeans et al., 2020; Moras et al. 2019; Pierson et al., 2011; D. Titze and Austin 2016; Wang et al., 2020; Yang et al., 2017; Yang et al., 2020). Previously unpublished data are available at <http://doi.org/10.5281/zenodo.4019639>.

## References

- Austin, J. A. (2019). Observations of radiatively driven convection in a deep lake. *Limnology & Oceanography*, 64(5), 2152–2160
- Bergstedt, R. A., Argyle, R. L., Seelye, J. G., Scribner, K. T., & Curtis, G. L. (2003). In situ determination of the annual thermal habitat use by lake trout (*Salvelinus namaycush*) in Lake Huron. *Journal of Great Lakes Research*, 29, 347–361. [https://doi.org/10.1016/S0380-1330\(03\)70499-7](https://doi.org/10.1016/S0380-1330(03)70499-7)
- Blanchfield, P. J., Tate, L. S., Plumb, J. M., Acolas, M. L., & Beaty, K. G. (2009). Seasonal habitat selection by lake trout (*Salvelinus namaycush*) in a small Canadian shield lake: Constraints imposed by winter conditions. *Aquatic Ecology*, 43(3), 777–787. <https://doi.org/10.1007/s10452-009-9266-3>
- Block, B. D., Denfeld, B. A., Stockwell, J. D., Flaim, G., Grossart, H. P. F., Knoll, L. B., & Sadro, S. (2019). The unique methodological challenges of winter limnology. *Limnology and Oceanography: Methods*, 17(1), 42–57. <https://doi.org/10.1002/lom3.10295>
- Boehrer, B., & Schultze, M. (2008). Stratification of lakes. *Reviews of Geophysics*, 46(2), RG2005. <https://doi.org/10.1029/2006RG000210>
- Bouffard, D., Zdorovenova, G., Bogdanov, S., Efreanova, T., Lavanchy, S., Palshin, N., & Zdorovenov, R. (2019). Under-ice convection dynamics in a boreal lake. *Inland Waters*, 9(2), 142–161. <https://doi.org/10.1080/20442041.2018.1533356>
- Brandt, S. B., Magnuson, J. J., & Crowder, L. B. (1980). Thermal habitat partitioning by fishes in Lake Michigan. *Canadian Journal of Fisheries and Aquatic Sciences*, 37(10), 1557–1564
- Bruesewitz, D. A., Carey, C. C., Richardson, D. C., & Weathers, K. C. (2015). Under-ice thermal stratification dynamics of a large, deep lake revealed by high-frequency data. *Limnology & Oceanography*, 60(2), 347–359. <https://doi.org/10.1005/lno.10014>
- Cannon, D. J., Troy, C. D., Liao, Q., & Bootsma, H. A. (2019). Ice-free radiative convection drives spring mixing in a large lake. *Geophysical Research Letters*, 46(12), 6811–6820. <https://doi.org/10.1029/2019GL082916>
- Charnock, H. (1955). Wind stress on a water surface. *Quarterly Journal of the Royal Meteorological Society*, 81(350), 639–640. <https://doi.org/10.1002/qj.49708135027>
- Chen, C. T. A., & Millero, F. J. (1986). Thermodynamic properties for natural waters covering only the limnological range. *Limnology & Oceanography*, 31(3), 657–662. <https://doi.org/10.4319/lno.1986.31.3.0657>
- Coman, M. A., & Wells, M. G. (2012). Temperature variability in the nearshore benthic boundary layer of Lake Opeongo is due to wind-driven upwelling events. *Canadian Journal of Fisheries and Aquatic Sciences*, 69(2), 282–296. <https://doi.org/10.1139/f2011-167>
- Cortés, A., & MacIntyre, S. (2019). Mixing processes in small arctic lakes during spring. *Limnology & Oceanography*, 65(2), 260–288. <https://doi.org/10.1002/lno.11296>
- Cote, D., Tibble, B., Curry, R. A., Peake, S., Adams, B. K., Clarke, K. D., & Perry, R. (2020). Seasonal and diel patterns in activity and habitat use by brook trout (*Salvelinus fontinalis*) in a small Newfoundland lake. *Environmental Biology of Fishes*, 103(1), 31–47. <https://doi.org/10.1007/s10641-019-00931-1>
- Cott, P. A., Guzzo, M. M., Chapelsky, A. J., Milne, S. W., & Blanchfield, P. J. (2015). Diel bank migration of Burbot (*Lota lota*). *Hydrobiologia*, 757(1), 3–20. <https://doi.org/10.1007/s10750-015-2257-6>
- Crawford, G. B., & Collier, R. W. (2007). Long-term observations of deepwater renewal in Crater Lake, Oregon. *Hydrobiologia*, 574(1), 47–68. <https://doi.org/10.1007/s10750-006-0345-3>
- Desai, A. R., Austin, J. A., Bennington, V., & McKinley, G. A. (2009). Stronger winds over a large lake in response to weakening air-to-lake temperature gradient. *Nature Geoscience*, 2(12), 855–858. <https://doi.org/10.1038/ngeo693>
- Fang, X., & Stefan, H. G. (1996). Dynamics of heat exchange between sediment and water in a lake. *Water Resources Research*, 32(6), 1719–1727. <https://doi.org/10.1029/96WR00274>
- Fang, X., & Stefan, H. G. (1998). Temperature variability in lake sediments. *Water Resources Research*, 34(4), 717–729. <https://doi.org/10.1029/97WR03517>

### Acknowledgments

The authors thank the Global Lake Ecological Observatory Network for organizing the GLEON 21 meeting, where this work was initially conceived. B. Yang and M. G. Wells acknowledges support from the Ontario Ministry of Environment, Conservation, and Parks (Grant LS-14-15-011) and the NSERC Discovery program (Grant RGPIN-2016-06542). The Lake Superior observations were supported by National Science Foundation Division of Ocean Sciences grant OCE-0825633 and NSF RAPID (Grant OCE-1445567). A. Laas acknowledges support from the Estonian Research Council Grant PSG32. G. A. Weyhenmeyer acknowledges the Swedish Infrastructure for Ecosystem Science (SITES) for provisioning of data from Lake Erken. SITES receives funding through the Swedish Research Council under the grant 2017-00635. Lake Mendota and Crystal Bog observations were supported by the US National Science Foundation grant DEB-1440297 and grant DEB-1856224. RMP acknowledges support from US National Science Foundation grants DEB 17276 and DEB 1950170. C. C. Carey acknowledges support from US National Science Foundation grant DEB 1753639 and 1933016. RMP acknowledges support from US National Science Foundation grants DEB 1754265, DEB 1754276, DEB 1950170. The data for the Pocono lakes were collected with support from Craig Williamson's Global Change Limnology Laboratory and Miami University, and from Kevin Rose's Global Water Laboratory at Rensselaer Polytechnic Institute. Alexie Lake data collections were supported by DeBeers Canada and Fisheries & Oceans Canada.

- Farmer, D. M., & Carmack, E. (1981). Wind mixing and restratification in a lake near the temperature of maximum density. *Journal of Physical Oceanography*, 11(11), 1516–1533. [https://doi.org/10.1175/1520-0485\(1981\)011<1516:WMARIA>2.0.CO;2](https://doi.org/10.1175/1520-0485(1981)011<1516:WMARIA>2.0.CO;2)
- Fee, E. J., Hecky, R. E., Kasian, S. E. M., & Cruikshank, D. R. (1996). Effects of lake size, water clarity, and climatic variability on mixing depths in Canadian Shield lakes. *Limnology & Oceanography*, 41(5), 912–920. <https://doi.org/10.4319/lo.1996.41.5.0912>
- Forrest, A. L., Laval, B. E., Pieters, R., & SS Lim, D. (2013). A cyclonic gyre in an ice-covered lake. *Limnology & Oceanography*, 58(1), 363–375. <https://doi.org/10.4319/lo.2013.58.1.0363>
- Gorham, E., & Boyce, F. M. (1989). Influence of lake surface area and depth upon thermal stratification and the depth of the summer thermocline. *Journal of Great Lakes Research*, 15(2), 233–245. [https://doi.org/10.1016/S0380-1330\(89\)71479-9](https://doi.org/10.1016/S0380-1330(89)71479-9)
- Guzzo, M. M., Blanchfield, P. J., Chapelsky, A. J., & Cott, P. A. (2016). Resource partitioning among top-level piscivores in a sub-Arctic lake during thermal stratification. *Journal of Great Lakes Research*, 42(2), 276–285. <https://doi.org/10.1016/j.jglr.2015.05.014>
- Hampton, S. E., Galloway, A. W., Powers, S. M., Ozersky, T., Woo, K. H., Batt, R. D., & Stanley, E. H. (2017). Ecology under lake ice. *Ecology Letters*, 20(1), 98–111. <https://doi.org/10.1111/ele.12699>
- Hampton, S. E., Moore, M. V., Ozersky, T., Stanley, E. H., Polashenski, C. M., & Galloway, A. W. (2015). Heating up a cold subject: Prospects for under-ice plankton research in lakes. *Journal of Plankton Research*, 37(2), 277–284. <https://doi.org/10.1093/plankt/fbv002>
- Harrison, P. M., Gutowsky, L. F. G., Martins, E. G., Patterson, D. A., Cooke, S. J., & Power, M. (2016). Temporal plasticity in thermal-habitat selection of burbot *Lota lota* a diel-migrating winter-specialist. *Journal of Fish Biology*, 88(6), 2111–2129. <https://doi.org/10.1111/jfb.12990>
- Hsu, S. A., Meindl, E. A., & Gilhousen, D. B. (1994). Determining the power-law wind-profile exponent under near-neutral stability conditions at sea. *Journal of Applied Meteorology*, 33(6), 757–765. [https://doi.org/10.1175/1520-0450\(1994\)033<0757:DTPLWP>2.0.CO;2](https://doi.org/10.1175/1520-0450(1994)033<0757:DTPLWP>2.0.CO;2)
- Huey, R. B. (1991). Physiological consequences of habitat selection. *The American Naturalist*, 137, S91–S115. <https://doi.org/10.1086/285141>
- Kelley, D. E. (1997). Convection in ice-covered lakes: Effects on algal suspension. *Journal of Plankton Research*, 19(12), 1859–1880. <https://doi.org/10.1093/plankt/19.12.1859>
- Kirillin, G., Leppäranta, M., Terzhevik, A., Granin, N., Bernhardt, J., Engelhardt, C., & Zdrovennova, G. (2012). Physics of seasonally ice-covered lakes: A review. *Aquatic Sciences*, 74(4), 659–682. <https://doi.org/10.1007/s00027-012-0279-y>
- Kirillin, G., & Shatwell, T. (2016). Generalized scaling of seasonal thermal stratification in lakes. *Earth-Science Reviews*, 161, 179–190. <https://doi.org/10.1016/j.earscirev.2016.08.008>
- Lewis, W. M., Jr (1983). A revised classification of lakes based on mixing. *Canadian Journal of Fisheries and Aquatic Sciences*, 40(10), 1779–1787. <https://doi.org/10.1139/f83-207>
- LSPA, Weathers, K. C., & Steele, B. G. (2020). High-frequency weather data at lake sunapee, New Hampshire, USA, 2007–2019 ver 3. *Environmental data initiative*. <https://doi.org/10.6073/pasta/698e9ffb0cddca81ecf7188bff54445e>
- MacKay, M. D., Verseghy, D. L., Fortin, V., & Rennie, M. D. (2017). Wintertime simulations of a boreal lake with the Canadian Small Lake Model. *Journal of Hydrometeorology*, 18(8), 2143–2160. <https://doi.org/10.1175/JHM-D-16-0268.1>
- Markfort, C. D., Perez, A. L., Thill, J. W., Jaster, D. A., Porté-Agel, F., & Stefan, H. G. (2010). Wind sheltering of a lake by a tree canopy or bluff topography. *Water Resources Research*, 46(3), W03530. <https://doi.org/10.1029/2009WR007759>
- McMeans, B. C., McCann, K. S., Guzzo, M. M., Bartley, T. J., Bieg, C., Blanchfield, P. J., & Ridgway, M. S. (2020). Winter in water: Differential responses and the maintenance of biodiversity. *Ecology Letters*, 23(6), 922–938. <https://doi.org/10.1111/ele.13504>
- Moras, S., Ayala, A. I., & Pierson, D. (2019). Historical modeling of changes in Lake Erken thermal conditions. *Hydrology and Earth System Sciences*, 23(12), 5001–5016. <https://doi.org/10.5194/hess-23-5001-2019>
- O'Reilly, C. M., Sharma, S., Gray, D. K., Hampton, S. E., Read, J. S., Rowley, R. J., & Weyhenmeyer, G. A. (2015). Rapid and highly variable warming of lake surface waters around the globe. *Geophysical Research Letters*, 42(24), 10773–10781. <https://doi.org/10.1002/2015GL066235>
- Pasche, N., Hofmann, H., Bouffard, D., Schubert, C. J., Lozovik, P. A., & Sobek, S. (2019). Implications of river intrusion and convective mixing on the spatial and temporal variability of under-ice CO<sub>2</sub>. *Inland Waters*, 9(2), 162–176. <https://doi.org/10.1080/20442041.2019.1568073>
- Pierson, D. C., Weyhenmeyer, G. A., Arvola, L., Benson, B., Blenckner, T., Kratz, T., & Weathers, K. (2011). An automated method to monitor lake ice phenology. *Limnology and Oceanography: Methods*, 9(2), 74–83. <https://doi.org/10.4319/lom.2010.9.0074>
- Pryor, S. C., Barthelmie, R. J., Young, D. T., Takle, E. S., Arritt, R. W., Flory, D., & Roads, J. (2009). Wind speed trends over the contiguous United States. *Journal of Geophysical Research: Atmosphere*, 114(D14), D14105. <https://doi.org/10.1029/2008JD011416>
- Read, J. S., Hamilton, D. P., Desai, A. R., Rose, K. C., MacIntyre, S., Lenters, J. D., & Rusak, J. A. (2012). Lake-size dependency of wind shear and convection as controls on gas exchange. *Geophysical Research Letters*, 39(9), L09405. <https://doi.org/10.1029/2012GL051886>
- Spigel, R. H., & Imberger, J. (1980). The classification of mixed-layer dynamics of lakes of small to medium size. *Journal of Physical Oceanography*, 10(7), 1104–1121. [https://doi.org/10.1175/1520-0485\(1980\)010<1104:TCOMLD>2.0.CO;2](https://doi.org/10.1175/1520-0485(1980)010<1104:TCOMLD>2.0.CO;2)
- Suski, C. D., & Ridgway, M. S. (2009). Seasonal pattern of depth selection in smallmouth bass. *Journal of Zoology*, 279(2), 119–128. <https://doi.org/10.1111/j.1469-7998.2009.00595.x>
- Titze, D. J., & Austin, J. A. (2014). Winter thermal structure of Lake Superior. *Limnology & Oceanography*, 59(4), 1336–1348. <https://doi.org/10.4319/lo.2014.59.4.1336>
- Titze, D., & Austin, J. (2016). Novel, direct observations of ice on Lake Superior during the high ice coverage of winter 2013–2014. *Journal of Great Lakes Research*, 42(5), 997–1006. <https://doi.org/10.1016/j.jglr.2016.07.026>
- Vautard, R., Cattiaux, J., Yiou, P., Thépaut, J. N., & Ciais, P. (2010). Northern Hemisphere atmospheric stilling partly attributed to an increase in surface roughness. *Nature Geoscience*, 3(11), 756–761. <https://doi.org/10.1038/ngeo979>
- Verpoorter, C., Kutser, T., Seekell, D. A., & Tranvik, L. J. (2014). A global inventory of lakes based on high-resolution satellite imagery. *Geophysical Research Letters*, 41(18), 6396–6402. <https://doi.org/10.1002/2014GL060641>
- Wang, J., Huang, L., Ju, J., Daut, G., Ma, Q., Zhu, L., & Graves, K. (2020). Seasonal stratification of a deep, high-altitude, dimictic lake: Nam Co, Tibetan Plateau. *Journal of Hydrology*, 584, 124668. <https://doi.org/10.1016/j.jhydrol.2020.124668>
- Wetzel, R. G. (2001). *Limnology: Lake and river ecosystems*, (pp. 93–128). Gulf Professional Publishing.
- Wüest, A., & Lorke, A. (2003). Small-scale hydrodynamics in lakes. *Annual Review of Fluid Mechanics*, 35(1), 373–412. <https://doi.org/10.1146/annurev.fluid.35.101101.161220>
- Yang, B., Wells, M. G., Li, J., & Young, J. (2020). Mixing, stratification, and plankton under lake-ice during winter in a large lake: Implications for spring dissolved oxygen levels. *Limnology & Oceanography*, 65(11), 2713–2729. <https://doi.org/10.1002/lno.11543>
- Yang, B., Young, J., Brown, L., & Wells, M. (2017). High-frequency observations of temperature and dissolved oxygen reveal under-ice convection in a large lake. *Geophysical Research Letters*, 44(24), 12218–12226. <https://doi.org/10.1002/2017GL075373>